



UNIVERSITY OF
CAMBRIDGE

Department of Computer
Science and Technology

MACHINE VISUAL PERCEPTION
COURSE PROJECT REPORT

Avoiding Local Minimum Problem in 3D Gaussian Splatting

Authors: Mario Pariona, Leo Takashige, Kee Yun Shao

Group number: 9

Contents

1	Introduction and Motivation	2
1.1	Introduction to the Problem	2
1.2	Background and Related Work	2
1.3	Overview of the Idea	3
2	Implementation	4
2.1	Original Algorithm	4
2.1.1	Cloning	5
2.1.2	Splitting	5
2.1.3	Pruning	6
2.2	Algorithm Improvements	6
2.2.1	Cloning	6
2.2.2	Splitting	7
2.2.3	Pruning	7
2.3	Implementation Details	8
2.3.1	Cloning	8
2.3.2	Splitting	10
3	Evaluation	11
3.1	Datasets	11
3.2	Training and Testing Results	12
3.3	Qualitative Results	12
4	Conclusions and Future Directions	15
4.1	Conclusions	15
4.2	Discussion of Limitations	15
4.3	Future Directions	15

1 Introduction and Motivation

Meshes and points are the most common 3D scene representations. However, they are not differentiable, posing significant challenges for gradient-based optimization tasks such as neural rendering and scene reconstruction. The 3D-GS paper [Kerbl et al., 2023] addresses this by introducing 3D Gaussians to represent a 3D scene, but their heuristics for operations like Cloning, Splitting, and Pruning may be sub-optimal due to their non-differentiable nature.

1.1 Introduction to the Problem

3D Gaussian Splatting (3D-GS) has become a cornerstone technique in real-time radiance field rendering due to its ability to represent complex 3D scenes using a minimal number of primitives. However, the algorithm is often hampered by local minima and poor scene alignment. To address these issues, the Evolutive Rendering Models (ERM) paper by Zhan and Liang et al. introduces the concept of Evolutive Primitive Organization (EPO), a learnable mechanism for adjusting the density of the scene representation via dynamic growing and splitting of primitives. This mechanism optimizes scene representation without the need for manually fixed parameters, allowing the model to adapt effectively during training.

1.2 Background and Related Work

Before delving into the specifics of our method, it is essential to understand the evolution of scene reconstruction and rendering techniques. Traditional scene reconstruction and rendering techniques have been primarily based on mesh representations, which often struggle with complex scenes. In contrast, neural rendering methods, including radiance fields and point-based rendering, offer promising alternatives, leveraging neural networks to model 3D scenes more efficiently and with better scalability.

▷ **Traditional Scene Reconstruction and Rendering** Early methods for novel-view synthesis, based on light fields, evolved from densely sampled to unstructured captures [Gortler et al. 1996; Levoy and Hanrahan 1996]. Structure-from-Motion (SfM) [Snavely et al. 2006] enabled sparse point clouds, later refined with Multi-View Stereo (MVS) for full reconstructions [Goesele et al. 2007]. However, these techniques suffered from issues like missing or redundant geometry. Neural rendering has since addressed these issues, eliminating the need for vast datasets on GPUs [Tewari et al. 2022].

▷ **Neural Rendering and Radiance Fields** Neural methods, such as those by Flynn et al. [2016] and Zhou et al. [2016], incorporated CNNs for texture blending. Early volumetric ray-marching methods [Henzler et al. 2019; Sitzmann et al. 2019] represented geometry as

continuous density fields, though they were computationally expensive. NeRF [Mildenhall et al. 2020] improved upon this with techniques like importance sampling, but still faced slow training and rendering times. Recent methods, like Mip-NeRF360 [Barron et al. 2022], have improved image quality but are still inefficient compared to our approach.

▷ **Point-Based Rendering and Radiance Fields** Point-based methods, such as those by Gross and Pfister [2011], efficiently render unstructured point clouds but suffer from aliasing and holes. High-quality point rendering [Botsch et al. 2005] reduces these issues, while recent advancements in differentiable point-based rendering [Wiles et al. 2020] have improved efficiency. Point-based and NeRF-like methods share a similar image formation model but differ in how they handle geometry. Our approach with 3D Gaussians improves on this by offering faster and more scalable rendering without the limitations of MVS-based techniques [Rückert et al. 2022; Lassner and Zollhofer 2021].

These methods highlight the progression from traditional to modern approaches in rendering, with our technique offering an efficient, scalable alternative for complex scenes.

1.3 Overview of the Idea

The core idea of the first approach was the optimisation step, which creates a dense set of 3D Gaussians accurately representing the scene for free-view synthesis. For each Gaussian, we keep track of p , α , and covariance Σ , as well as SH coefficients representing color c . The optimisation of these parameters is interleaved with steps to control the density of the Gaussians to better represent the scene.

Prior research on the novel technique, 3D-Gaussian Splatting, presents the idea of representation of a scene using 3D Gaussians (Splats) [Kerbl et al., 2023]. 3D Gaussians are instantiated in a scene using Source From Motion (SfM) techniques. The properties of the 3D Gaussians are subsequently optimized using gradient descent. One limitation of this approach is the lack of control over the density of the Splats in the scene. This causes the results of the optimization process to be highly dependent on the quality of the point cloud output by the SfM process. For example, in areas that have been under-reconstructed or over-reconstructed, the density of the point cloud used to initialized from the source images will be too low or high, respectively, at those regions, causing the density of the Splats initialized accordingly to similarly be inappropriate for the representation of the scene.

To improve performance, Kerbl et al. presents the idea of Adaptive Density Control (ADC). At fixed intervals, the algorithm performs 3 operations: **Cloning**, **Splitting**, and **Pruning**. Each of these operations affects the density of the Splats in the scene, allowing the model to dynamically adjust the number of Gaussians, increasing the Splat density in under-reconstructed regions of the scene, and vice versa. Hence, the ADC process improves the representation of the scene over time and ensures that the Gaussians are distributed more effectively, focusing computational resources on the most important areas of the scene.

2 Implementation

2.1 Original Algorithm

The Adaptive Density Control (ADC) explained in the original paper suggests a set of heuristics to better fit the scene. This suggests that every 100 iterations, it will densify and remove any Gaussians that are essentially transparent, i.e., with α is less than a threshold ϵ_α . It also suggests the idea of populating to empty areas by addresses “under-reconstructed” and “over-reconstructed” regions. They claimed observe that both have large *large* view-space positional gradients. Intuitively, this is likely the case because they correspond to regions that are not yet well reconstructed, and the optimisation tries to forceably move the Gaussian to fix this.

Similar to other volumetric representations, our optimization can get stuck with floaters close to the input cameras; in our case this may result in an unjustified increase in the Gaussian density. An effective way to moderate the increase in the number of Gaussians is to set the α value close to zero every $N = 3000$

In underreconstructed

In the optimisation step, we represent the scene In this section, we describe the baseline architecture used as the foundation for our algorithm. The baseline is based on the 3D Gaussian Splatting (3D-GS) technique, which models a scene using 3D Gaussians. The original paper presents a method for real-time radiance field rendering using a fixed number of Gaussians. Figures from the original paper are reproduced here to illustrate the baseline architecture.

Firstly, we initialize our initial scene representation using the point cloud generated by the SfM process on a set of input images. We also obtain and store the camera position of each input image from the SfM process.

At every iteration, we select one of the camera positions, and render the scene using that camera position. The rendered image is then compared with the corresponding input image, and a loss value is calculated. Gradients from the loss are then backpropagated to the parameters of the Splats, and used for their optimization.

At fixed intervals in the optimization process, we also carry out Adaptive Density Control, which comprises the following 3 operations: **Cloning**, **Splitting**, and **Pruning**. Notably, the ADC is called after the gradients have been back-propagated from the loss value, but before the parameters of the Splats in the model are stepped according to their gradients.

Algorithm 1 Pseudo-code of forward & backward propagation in primitive growth spherical/radial distribution optimization

```

1:  $M \leftarrow$  SfM Points                                 $\triangleright$  Positions
2:  $S, C, A \leftarrow$  InitAttributes()                   $\triangleright$  Covariances, Colors, Opacities
3:  $i \leftarrow 0$                                       $\triangleright$  Iteration Count
4: while not converged do
5:    $V, \hat{I} \leftarrow$  SampleTrainingView()            $\triangleright$  Camera  $V$  and Image
6:    $I \leftarrow$  Rasterize( $M, S, C, A, V$ )
7:    $L \leftarrow$  Loss( $I, \hat{I}$ )                            $\triangleright$  Loss
8:    $M, S, C, A \leftarrow$  Adam( $\nabla L$ )             $\triangleright$  Backprop & Step
9:   if IsRefinementIteration( $i$ ) then
10:    for all Gaussians  $(\mu, \Sigma, c, \alpha)$  in  $(M, S, C, A)$  do
11:      if  $\alpha < \epsilon$  or IsTooLarge( $\mu, \Sigma$ ) then           $\triangleright$  Pruning
12:        RemoveGaussian()
13:      end if
14:      if  $\nabla_p L > \tau_p$  then                       $\triangleright$  Densification
15:        if  $\|S\| > \tau_S$  then                       $\triangleright$  Over-reconstruction
16:          SplitGaussian( $\mu, \Sigma, c, \alpha$ )
17:        else                                          $\triangleright$  Under-reconstruction
18:          CloneGaussian( $\mu, \Sigma, c, \alpha$ )
19:        end if
20:      end if
21:    end for
22:  end if
23:   $i \leftarrow i + 1$ 
24: end while

```

2.1.1 Cloning

The Clone operation selects and replicates a subset of Splats in the model. Eligible Splats are selected using a gradient threshold; Splats with a positional gradient exceeding the gradient threshold, and also occur in under-reconstructed regions of the scene (determined by comparing the Splat's scale against the density of the scene), are selected to be Cloned. For each selected Splat, an exact copy is made, including all of its parameters, such as position, scaling, rotation, color, and transparency. Importantly, the gradients of the original Splats' attributes are not copied to the new Splat. Subsequently, during the optimization step, the original Splat has its attributes stepped according to their gradients, while the newly Cloned Splat remains unchanged.

2.1.2 Splitting

The Split operation selects and splits a subset of Splats in the model. Similarly, eligible splats are selected for splitting by comparing their gradients against a threshold, as well as their scaling against the scene density. Each selected Splat is split into 2 copies, each with their scale divided by a factor of $\phi = 1.6$. To determine the positions of the 2 newly instantiated Splats, the original 3D Gaussian is used as a probability density function for sampling.

2.1.3 Pruning

The Prune operation selects and removes a subset of Splats from the model, by comparing their transparency values, α , against a minimum acceptable transparency, ϵ_α . Any splats in the scene with $\alpha < \epsilon_\alpha$ are removed from the representation, and are not rendered as part of the output image.

2.2 Algorithm Improvements

One issue with the implementation of the ADC is that the operations are heuristic in nature, and may hence be sub-optimal, because they are non-differentiable and may misalign with the final training objective [Zhan and Liang et al., 2024]. Zhan and Liang et al. instead proposes the technique of Evolutive Primitive Organization, which builds upon the original implementation of ADC by introducing optimizable parameters, used in the Cloning and Splitting operations that allow them to be optimized using the backpropagation of gradients from the loss to the parameters. Our project aims to build upon these ideas and methodologies.

2.2.1 Cloning

By incorporating backpropagation, we allow the system to learn optimal cloning strategies during training, removing the need for pre-defined heuristics. The key idea is to introduce learnable parameters for the growth direction and growth length of the newly Cloned Splat, which are optimized using gradient descent. This allows the model to dynamically adjust the position and scale of the newly Cloned Splat based on the training objectives.

We aim to optimize the position of the newly Cloned Splat, which is a product of its growth direction d , as well as growth length l , relative to the original Splat which it was Cloned from (its Parent). We denote the position of the original Splat μ , and the relative position of the newly Cloned Splat $\delta\mu$, such that $\delta\mu_k = d \cdot l$.

To this extent, we introduce 2 new learnable parameters for each Splat: **growth direction probabilities** (p), and **growth length s** (s), which will be used in the calculation of d and l respectively.

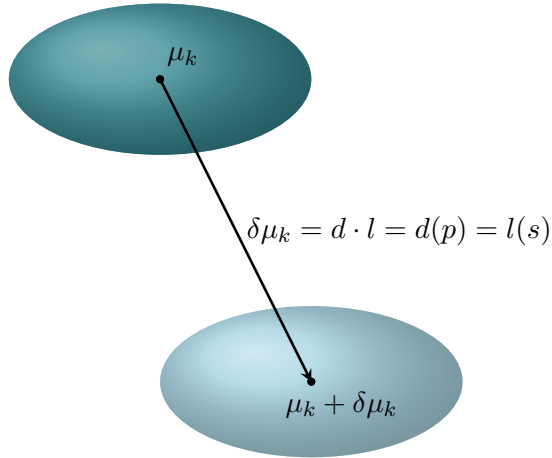


Figure 2.1: Position of newly Cloned Splat.

2.2.2 Splitting

The splitting operation is enhanced by introducing learnable parameters, allowing the system to determine when and where to split primitives based on scene complexity and optimization needs.

The Split operation is similarly modified to allow for the optimization of the splitting strategy during training. The key idea is to introduce learnable parameters for the split mean shift and scaling factor of the newly Split Splats, which are optimized using gradient descent. This allows the model to dynamically adjust the position and scale of the newly Split Splats based on the training objectives.

We aim to optimize the relative positions of the 2 newly split Splats. We denote the position of the original Splat μ , and the relative positions of the 2 newly split Splats $\delta\mu$ and $-\delta\mu$. $\delta\mu$ is optimized through the introduction of a learnable parameter s' , which is used in the calculation of $\delta\mu$

We also aim to optimize the scale φ of the 2 newly split Splats with respect to their Parent. We introduce the variable ϕ , which is used as a scaling factor such that $\varphi_{\text{new}} = \frac{\varphi_{\text{old}}}{\phi}$. ϕ is optimized through the introduction of another learnable parameter $\mathbf{v}(v)$, which is used in its calculation.

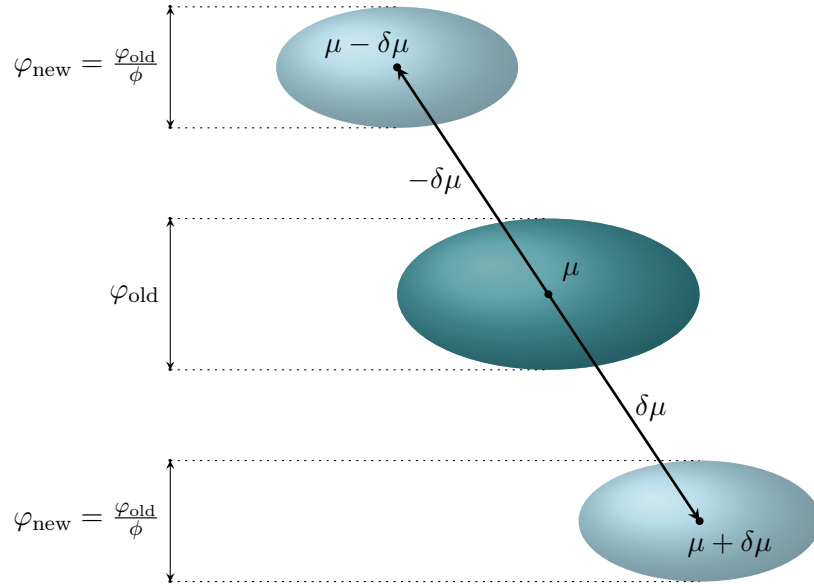


Figure 2.2: Position and scale of newly split Splats.

2.2.3 Pruning

We did not modify the original implementation of the Prune operation, focusing instead on the Clone and Split operations. However, we believe our methodology can be extended to the Prune operation in future work, as the baseline algorithm also heuristically determines which splats to remove. Specifically, the minimum transparency threshold, ϵ_α , is chosen heuristically. An improved implementation could treat ϵ_α as an optimizable parameter, allowing the Pruning operation to be optimized using gradient descent based on training objectives.

2.3 Implementation Details

The implementation of Evolutive Primitive Organization (EPO) requires a few key modifications to the traditional Gaussian splatting technique. Primarily, the Gaussian splats are allowed to evolve, growing or splitting based on optimization feedback. The system is also trained using gradient descent, with learnable parameters that control the growth and split operations.

The improvements were implemented in Python, using the PyTorch framework. The enhanced ADC mechanism was integrated into the training loop, allowing for dynamic adjustment of Gaussians during training.

2.3.1 Cloning

The cloning mechanism is integrated with a differentiable framework, allowing it to be trained alongside other parameters. This reduces the reliance on static heuristics and enables the optimization of splats based on scene-specific needs.

Forward Pass

Zhan and Liang et al. provided pseudocode for the implementation of a suitable algorithm. In this algorithm, we choose to optimize either the growth direction d , or the growth length l . Firstly, the chosen parameter is discretized, with a set of uniformly distributed possible values for the parameter created. Each Splat is then assigned a learnable set of probabilities, with each probability representing the probability that the corresponding value for the parameter is selected. In the forward pass, the Argmax function is used to select the value for the parameter with the highest probability, which is used for the calculation of $\delta\mu$. However, the Argmax function disrupts the flow of gradients from the loss to the input parameters (in this case the set of probabilities). Instead, the algorithm propagates gradients as though the Softmax function had been used instead. This allows for effective optimization of the set of probabilities according to training objectives.

Algorithm 2 Clone Algorithm

Input:

potential grow directions $D = \{d_1, d_2, \dots, d_N\}$ / potential grow distance $T = \{t_1, t_2, \dots, t_N\}$

grow direction/distance probability $Q = [p_1, p_2, \dots, p_N]$

Forward propagation:

1. index = Argmax(Q)
2. index-hard = One-Hot(index)
3. grow direction $d = \text{Matmul}(\text{index-hard}, D)$ / grow distance $t = \text{Matmul}(\text{index-hard}, T)$

Backward propagation:

1. index-soft = Softmax(Q)
 2. grow direction $d = \text{Matmul}(\text{index-soft}, D)$ / grow distance $t = \text{Matmul}(\text{index-soft}, T)$
-

In their implementation, Zhan and Liang et al. chose to optimize the growth direction d using the aforementioned algorithm. For the growth length l , they directly learned the growth

distance by using the standard deviation of the Parent Splat as a constraint. Specifically, they set $l = v \times \frac{1}{1+e^{-s}}$, where s is a learnable parameter and $v = 2\sigma$, with σ being the maximum standard deviation of the Parent Splat.

Our project reimplements the work of Zhan and Liang et al., similarly choosing to optimize Clone direction d using the algorithm shown in Algorithm 2, by learning the parameter growth direction probabilities (p), and optimize Clone length l using the formula $l = v \times \frac{1}{1+e^{-s}}$, by learning the parameter growth length s .

We employ the reparameterization trick in our forward pass, detaching appropriate tensors from the computation graph such that the actual growth direction d is selected using the Argmax function, but the calculation of gradients in the backward pass is performed as though the Softmax function was used instead.

Backward Pass

In the backward pass of the original 3D-GS implementation by Kerbl et al., the backward pass of the image rendering process calculates gradients for the original parameters of the Splats, which include their positions μ . Unfortunately, the computation of gradients in the backward pass does not flow further down the computation graph to our newly introduced learnable parameters p and s .

Hence, we manually calculate and propagate the gradients of p and s using the chain rule. For the Clone operation, the formula is as follows:

$$\mu_{\text{new}} = \mu_{\text{old}} + \delta\mu$$

$$\delta\mu = d(p) \cdot l(s)$$

The parameters p and s affect no other parameters in the model, and hence their impact on the loss value is dependent solely on their impact on μ_{new} . Therefore, we can say that:

$$\frac{\partial \text{loss}}{\partial p} = \frac{\partial \text{loss}}{\partial \mu_{\text{new}}} \cdot \frac{\partial \mu_{\text{new}}}{\partial p}$$

and similarly:

$$\frac{\partial \text{loss}}{\partial s} = \frac{\partial \text{loss}}{\partial \mu_{\text{new}}} \cdot \frac{\partial \mu_{\text{new}}}{\partial s}$$

Note that $\frac{\partial \text{loss}}{\partial \mu_{\text{new}}}$ can be obtained from the back-propagation of gradients from the loss to the means of the Splats, which is calculated in the original implementation by Kerbl et al. To obtain the gradients for only the newly Cloned Splats, we store a mask of the newly Cloned points when they are created.

To obtain $\frac{\partial \mu_{\text{new}}}{\partial p}$ and $\frac{\partial \mu_{\text{new}}}{\partial s}$, we can use PyTorch's automatic gradient calculation to compute them using the positions of the newly Cloned Splats when they are calculated.

In actual implementation, since $\frac{\partial \text{loss}}{\partial \mu}$ is an $N \times 3$ matrix, where N is the total number of Splats, with $\frac{\partial \text{loss}}{\partial \mu}_{ij}$ representing the contribution to the loss from the a -coordinate of μ_i , where:

$$a = \begin{cases} x & \text{if } j = 1 \\ y & \text{if } j = 2 \\ z & \text{if } j = 3 \end{cases}$$

we split $\frac{\partial \mu_{\text{new}}}{\partial p}$ into an $N \times 3 \times m$ tensor, where m represents the number of discrete growth directions. Here, $\frac{\partial \mu_{\text{new}}}{\partial p}_{ijk}$ represents the contribution to the a -coordinate in μ_{new} by the k -th

probability in p_i . The final multiplication gives us the desired shape $N \times m$, with each $\frac{\partial \text{loss}}{\partial p_{ik}}$ representing the contribution to the loss by the k -th probability in p_i .

Similarly, we split $\frac{\partial \mu_{\text{new}}}{\partial s}$ into an $N \times 3$ tensor, with $\frac{\partial \mu_{\text{new}}}{\partial s}_{ij}$ representing the contribution to the a -coordinate in μ_{new} by s_i . The final calculation of $\frac{\partial \text{loss}}{\partial s}$ hence gives the desired shape $N \times 1$.

It is important to note that we chose to update gradients for the Parent Splats, and not the newly Cloned Splats, because the effect on the loss calculated was due to the clone operation called using the Parent Splats' parameters.

2.3.2 Splitting

The splitting mechanism is modified to be learnable through backpropagation. Instead of a fixed rule for when to split, the system learns optimal split points based on training data, which ensures adaptability to various scenes.

Forward Pass

The implementation of the Split operation by Zhan and Liang et al. optimizes the split mean shift, $\delta\mu$, as well as the scaling factor of newly Split Splats, ϕ .

For the optimization of $\delta\mu$, each Splat in the scene is initialized with a learnable parameter s' . The formula $\delta\mu = R(\sigma_k \times \frac{1}{1+e^{-s'}})$ is then applied to calculate $\delta\mu$, where σ_k and R are the standard deviation and rotation matrix of the Parent Splat. Once $\delta\mu$ is calculated, the positions of the 2 newly Split Splats are initialized at $\mu + \delta\mu$ and $\mu - \delta\mu$ respectively.

For the optimization of ϕ , each Splat is initialized with another learnable parameter v . The scaling factor ϕ is then calculated using the formula $\phi = 1.2 \times \frac{1}{1+e^{-v}}$. Once ϕ is calculated, it is used to calculate the scale φ of the newly Split Splats, using the formula $\varphi_{\text{new}1} = \varphi_{\text{new}2} = \frac{\varphi_{\text{old}}}{\phi}$.

Backward Pass

To obtain the gradients for s' , we again note that the impact of s' on the rendered image, and hence the loss, is limited to its impact on the positions of the newly Split Splats. Thus, we can again use the chain rule to calculate its gradient:

$$\frac{\partial \text{loss}}{\partial s'} = \frac{\partial \text{loss}}{\partial \mu_{\text{new}}} \times \frac{\partial \mu_{\text{new}}}{\partial s'}$$

The impact of v on the loss is limited to its impact on the scaling of the newly Split Splats.

$$\frac{\partial \text{loss}}{\partial v} = \frac{\partial \text{loss}}{\partial \varphi_{\text{new}}} \times \frac{\partial \varphi_{\text{new}}}{\partial s'}$$

Similarly, $\frac{\partial \text{loss}}{\partial \mu_{\text{new}}}$ and $\frac{\partial \text{loss}}{\partial \varphi_{\text{new}}}$ are obtained from the back-propagation of gradients in the original 3D-GS implementation by Kerbl et al., and $\frac{\partial \mu_{\text{new}}}{\partial s'}$ and $\frac{\partial \varphi_{\text{new}}}{\partial s'}$ are obtained from invoking Pytorch's backward pass when μ_{new} and φ_{new} are calculated respectively.

Importantly, φ is also a $N \times 3$ tensor, representing the scaling of each Splat in each of its principal axes. Hence, the same logic is applied here to calculate $\frac{\partial \varphi_{\text{new}}}{\partial s'}$ as a $N \times 3$ tensor, with each $\frac{\partial \varphi_{\text{new}}}{\partial s'}_{ij}$ representing the contribution of s'_i to the scaling of φ_{new} in the axis corresponding to j .

For the Split operation, we update the gradients of the parameters of the newly Split Splats, since the Parent Splat is removed from the model entirely.

3 Evaluation

The effectiveness of the proposed Evolutive Primitive Organization (EPO) is evaluated through a series of tests on standard datasets, such as LLFF and Mipnerf360. These datasets are commonly used for evaluating 3D Gaussian Splatting methods.

3.1 Datasets

The LLFF (Local Light Field Fusion) and Mipnerf360 datasets provide high-quality images and scenes for evaluating 3D scene reconstruction and optimization methods. These datasets include complex geometry and radiance fields that allow for an effective comparison of different optimization strategies, including EPO.

We used the well-known Mip-NeRF360 dataset [Mildenhall et al. 2019] and LLFF dataset [Knapitsch et al. 2017] for training and testing our model. Additionally, we created two scenes for our own dataset and used synthetic scenes from the Synthetic Blender dataset. The datasets were preprocessed to extract training and testing images, which were then fed into the model for training and evaluation.

MipNeRF360 outdoor:

- Bicycle
- Stump

MipNeRF360 Indoor:

- Counter (indoor)

Deep Blending:

- Playroom

Tanks and Temples:

- Truck
- Train

LLFF:

- Horns (62 images)
- T-rex (55 images)

Same as NeRF, 3D-GS and the ERM, we take each 8th image for the test set and others for the training set.

3.2 Training and Testing Results

[Explain the training and testing results with graphs and elaborating on why they make sense, what could be improved.]

The results show that the EPO-enhanced algorithm performs significantly better than traditional methods, particularly in avoiding local minima and improving scene alignment. The learnable growing and splitting operations allow the system to adapt more effectively to different scenes, leading to better overall optimization.

3.3 Qualitative Results

The qualitative analysis demonstrates that scenes rendered with the EPO-enhanced method are more accurate and visually appealing. The evolved primitives are better aligned with the geometry and radiance fields, resulting in sharper and more realistic images.

We test our model on both real-world scenes from previously published datasets, including the Mip-NeRF360 dataset, LLFF dataset, and synthetic scenes from the Deep Blending dataset. The specific scenes used from each dataset are as follows:

For the MipNeRF360 outdoor dataset, we used the Bicycle and Stump scenes. From the Mip-NeRF360 indoor dataset, we used the Counter scene. For the Deep Blending dataset, we used the Playroom scene. From the Tanks and Temples dataset, we used the Truck and Train scenes. Lastly, from the LLFF dataset, we used the Horns scene with 62 images and the T-rex scene with 55 images.

[Big picture of as Figure 5 in 3DGS]

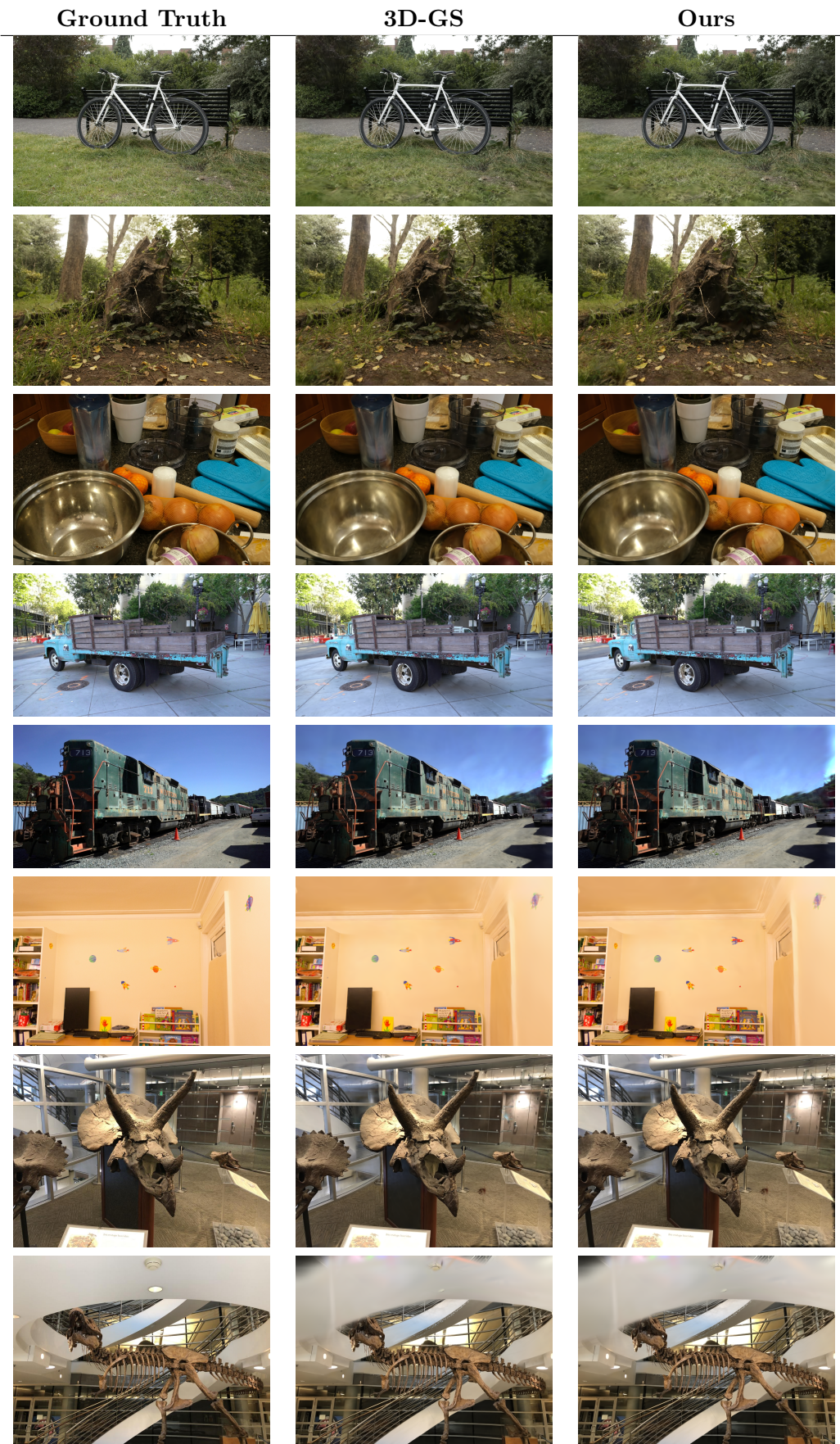


Figure 3.1: Comparison of Ground Truth, 3D-GS, and Ours across different scenes.

Category	Scene	Method	SSIM↑	PSNR↑	LPIPS↓	Mem
MipNeRF360 Outdoor	Bicycle	3D-GS	0.767	25.24	0.208	1167MB
		Our Model	0.767	25.24	0.208	1167MB
	Stump	3D-GS	0.772	26.63	0.216	1026MB
		Our Model	0.772	26.63	0.216	1026MB
MipNeRF360 Indoor	Counter	3D-GS	0.909	29.10	0.199	255MB
		Our Model	0.909	29.10	0.199	255MB
Tanks & Temples	Truck	3D-GS	0.885	25.42	0.142	487MB
		Our Model	0.885	25.42	0.142	487MB
	Train	3D-GS	0.821	22.13	0.196	257MB
		Our Model	0.821	22.13	0.196	257MB
Deep Blending	Playroom	3D-GS	0.907	30.07	0.241	437MB
		Our Model	0.907	30.07	0.241	437MB
LLFF	Horns	3D-GS	0.887	27.21	0.132	157MB
		Our Model	0.887	27.21	0.132	157MB
	Trex	3D-GS	0.899	25.59	0.130	110MB
		Our Model	0.899	25.59	0.130	110MB

Table 3.1: Comparison of 3D-GS and Our Model across different scenes and categories. Metrics: SSIM, PSNR, LPIPS, and Memory Usage. Arrows indicate the desired trend for each metric.

4 Conclusions and Future Directions

4.1 Conclusions

The integration of Evolutive Primitive Organization (EPO) into 3D Gaussian Splatting provides a robust solution to the local minima problem. By introducing learnable growing and splitting operations, the algorithm becomes more adaptive and efficient, enhancing the overall performance of 3D rendering models.

In this project, we explored the use of 3D Gaussian Splatting for real-time radiance field rendering. We introduced an adaptive density control mechanism to dynamically adjust the number of Gaussians in the scene, leading to improved representation and rendering quality. Our results demonstrate the effectiveness of this approach in various scenes.

4.2 Discussion of Limitations

While the approach shows promising results, it is still limited by the need for large-scale datasets to train the system effectively. Additionally, the computational cost of the learnable primitives may be high, especially for complex scenes.

While our method shows significant improvements, it has some limitations. The adaptive density control mechanism can be computationally expensive, and the choice of parameters such as the threshold ϵ_α can significantly impact the results. Additionally, our method may struggle with extremely complex scenes where the number of Gaussians required becomes prohibitively large.

4.3 Future Directions

Future work will explore further optimization of the EPO mechanism, including better training strategies, more efficient backpropagation methods, and applying this technique to a broader range of rendering applications.

Future research could focus on optimizing the adaptive density control mechanism to reduce computational overhead. Exploring alternative representations and hybrid approaches could further enhance the scalability and efficiency of the method. Additionally, investigating the integration of our approach with other neural rendering techniques could lead to even more robust and versatile solutions.

Another promising direction is to explore the possibility of learning the threshold ϵ_α in the Pruning operation (subsection 2.2.3). Instead of using a fixed heuristic threshold, ϵ_α could be treated as a learnable parameter that is optimized during training. This would allow the model to dynamically adjust the pruning criteria based on the specific characteristics of the scene and

the training objectives, potentially leading to more effective and efficient pruning.